Physica A 389 (2010) 3965–3971

Contents lists available at ScienceDirect

Physica A

journal homepage: www.elsevier.com/locate/physa

# Domain growth dynamics in multicomponent vesicles composed of BSM/DOPC/cholesterol

Xinyu Liang, Li Li, Feng Qiu *, Yuliang Yang **

*The Key Laboratory of Molecular Engineering of Polymers, Ministry of Education, Department of Macromolecular Science, Fudan University, Shanghai 200433, China*

ARTICLE INFO

*Article history:*
Received 5 February 2010
Received in revised form 27 May 2010
Available online 8 June 2010

*Keywords:*
Vesicle
Ternary mixture
Phase separation
Domain growth
Scaling law

ABSTRACT

We have investigated the domain growth dynamics in vesicles composed of BSM/DOPC/cholesterol using fluorescence microscopy. A ternary mixture of equimolar BSM, DOPC, and cholesterol was employed, and two fluorescent dyes were added for comparison studies. We found that in the early stage the number of the domains on the vesicle surface, $N(t)$, decayed with time as $N(t) \sim t^{-2/3}$, which confirmed previous theoretical prediction and numerical simulation, while in the late stage $N(t)$ decreased more quickly, as $\sim t^{-\beta}$, with $\beta \approx 2$. We discuss the faster growth dynamics based on the collision-induced collision mechanism.

© 2010 Elsevier B.V. All rights reserved.

## 1. Introduction

The lateral heterogeneity in biomembranes plays important roles in many cellular processes, such as sorting and trafficking of proteins, signal transduction, membrane fusion, and membrane budding [1–5]. In order to understand the mechanisms in the lateral organization and spatio-temporal dynamics of cell membranes, vesicles mainly composed of saturated phospholipids, unsaturated phospholipids, and cholesterol have been widely used as model systems. Saturated phospholipids usually have higher melting temperature, while unsaturated phospholipids have lower melting temperature, resulting in liquid-ordered phases ($L_o$) and liquid-disordered phases ($L_d$) below their miscibility transition temperatures, respectively. Thermodynamic ternary phase diagrams of various model membranes have been constructed [6–8], and the lateral diffusion coefficients of the lipids in such model membranes have also been determined [9–11]. Meanwhile, the correlation between the mechanical properties and the domain composition, as well as the geometry of the vesicles with coexisting $L_o$ and $L_d$ phases, has been studied [12–16].

Non-equilibrium states of fluid vesicles [17–23], which are more relevant to a dynamic cell, have also attracted attention. Theoretical models based on Ginzburg–Landau theory and computer simulations using Monte Carlo techniques and dissipative particle dynamics have been applied to describe the dynamic behavior of the phase separation of fluid membranes [18–23]. On the experimental side, Saeki et al. [24] reported the kinetics of domain growth in a vesicle composed of DPPC/DOPC/cholesterol, in which the average domain size, $r$, develops with time $t$ as $r \sim t^{0.15}$. However, for the same ternary mixture, Yanagisawa et al. [25] recently pointed out that the domain-coarsening processes can be categorized into two types, depending on the area-to-volume ratio of the vesicle: for the normal coarsening processes (usually with very low area-to-volume ratio), the average size of domains grows as a power law $r \sim t^{2/3}$; and for the trapped coarsening processes (usually with higher area-to-volume ratio), the domain coarsening is suppressed at a certain domain size. Such dynamically

* Corresponding author. Tel.: +86 21 5566 4036; fax: +86 21 6564 0293.
** Corresponding author.
*E-mail addresses:* fengqiu@fudan.edu.cn (F. Qiu), yuliangyang@fudan.edu.cn (Y. Yang).

0378-4371/$ – see front matter © 2010 Elsevier B.V. All rights reserved.
doi:10.1016/j.physa.2010.05.052

arrested states were also reported by Ursell et al. [26] and Semrau et al. [27], in which membrane-mediated repulsive forces were observed. All these earlier experiments reveal the important role of domain budding or dimpling on the domain growth dynamics: flat domains rapidly fuse until complete phase separation is attained, while two approaching budded domains distort the surrounding membrane, which induces repulsive interdomain interaction and thus hinders domain coalescence.

In a previous paper, we reported the budding dynamics of tubular vesicles composed of the ternary mixture DPPC/DOPC/cholesterol [28]. The large area-to-volume ratio of the tubular vesicles made the budding of domains much easier than that in spherical vesicles. We observed that in the late stage the number of buds, $N$, decayed monotonically with time, following a scaling law $N \sim t^{-2/3}$. This scaling relation differs from Saffman–Delbrück's result obtained from a simple model of protein molecules diffusing in lipid bilayer membranes [29], but agrees well with the computer simulations in which the solvent hydrodynamic effect and vesicle volume constraint were considered [21,22].

In this paper, we further investigate the domain growth dynamics in spherical vesicles composed of BSM/DOPC/cholesterol. We use BSM instead of DPPC because BSM has smaller head size compared to phosphocholines, leading to more thermodynamically stable domains. We observe that in the early stage the number of domains on the vesicle surface, $N$, decays with time as $N \sim t^{-2/3}$, which is consistent with previous theoretical prediction and numerical simulation [22]. However, in the late stage an acceleration of domain growth is observed and the scaling exponent changes from $-2/3$ to close to $-2$. The rapid growth of domains is attributed to the collision-induced collision mechanism that was found previously in binary fluid mixtures by Tanaka [30–32]. Furthermore, to compare the effect of fluorescent dye on the domain growth dynamics, both TR–DHPE and Chol–BODIPY were used in the experiment.

## 2. Experimental section

### 2.1. Materials

BSM (sphingomyelin, from bovine brain), DOPC (1,2-dioleoyl-sn-glycero-3-phosphocholine) and Chol (cholesterol) were purchased from Sigma-Aldrich (St. Louis, MO, USA). TR–DHPE (Texas Red–1,2-dihexadecanoyl-sn-glycero-3-phosphoethanolamine) and Chol–BODIPY (cholesteryl–4,4-difluoro-5,7-dimethyl-4-bora-3a,4a-diaza-s-indacene-3-dodecanoate) were purchased from Molecular Probes (Eugene, OR, USA). All the above reagents were used as supplied. Other solvents were at least analytical grade and were used without further purification. Milli-Q water with a resistivity of 18.2 M$\Omega$/cm was used in the experiment.

### 2.2. Preparation of vesicles

The vesicles were prepared according to the method described in [12]. Equimolar BSM, DOPC, and cholesterol (1:1:1) were dissolved in chloroform/methanol (9:1 v/v) to 0.8 mg/mL as stock solution and stored at 20 °C for later use. To enhance the image contrast between the two phases, a fluorescent dye was added into the mixture. In the case of TR–DHPE as the dye, the concentration was 0.3 wt% of TR–DHPE /lipid, while in the case of Chol–BODIPY, it was 2.0 wt% Chol–BODIPY/lipid. A droplet of the above solution, approximately 3 μL, was deposited on the center of a prewarmed glass slide, then covered with black paper and kept in vacuum at 55 °C overnight to remove the solvent. The dry film was then prehydrated under water-saturated $N_2$ at 55 °C for several hours until the film became transparent. After the glass slide was put onto a 55 °C heating stage, a tiny drop of water was dripped on the film for hydration and incubation for 20 min. After the vesicles formed, the sample was quenched to 15 °C (which was below the miscibility transition temperature of the ternary mixture) at a rate of 7 °C/min, and the phase separation was triggered after a while. The temperature of the system was equilibrated in seconds after the temperature quench. The starting point ($t = 0$) was chosen when phase separation was recognizable under the microscope. It was a time later than when the phase separation initiated. We did not observe any transient effects associated with the temperature quench in the experiments. To compare the effect of fluorescent dyes on the phase separation processes, instead of TR–DHPE, in some cases Chol–BODIPY was added into the same stock solution above.

### 2.3. Fluorescence microscopy

An epifluorescence microscope (BX51, Olympus, Japan), equipped with a 50× semi-achroplane objective (NA = 0.5, working distance = 10.6 mm) and a heating stage (±0.1 °C accuracy, THMS600, Linkam, England), was employed to investigate the phase separation of the spherical vesicles. The images were recorded by a CCD camera (Pixelink, Linkam, England) at a rate of 1 frame/s and analyzed by a Linksys32DV (Linkam, England).

## 3. Results and discussion

The ternary mixture BSM/DOPC/Chol with the composition 1:1:1 was chosen to produce spherical vesicles. After quenching the ternary mixture from the one-phase region into the liquid–liquid coexisting region, phase separations through either a nucleation-and-growth mechanism or a spinodal decomposition mechanism may occur, depending on the composition and temperature of the ternary mixture. With the aid of the fluorescent dye TR–DHPE, the phase-separation processes can be clearly recognized (see Fig. 1). The bright red phase (droplets) is the DOPC-rich $L_d$ phase, and the dark phase (continuous background) is the BSM-rich $L_o$ phase. It should be noted that in our system we always observe $L_d$ droplets in

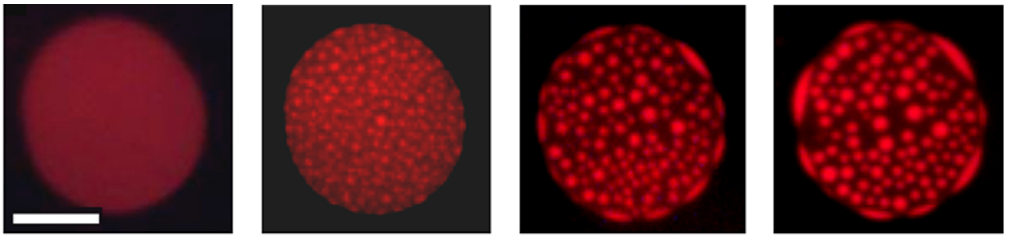

(a) 1 s. (b) 12 s. (c) 42 s. (d) 64 s.

**Fig. 1.** Time evolution of domain growth on the vesicle quenched from 55 °C to 15 °C. The bright red phase marked by TR–DHPE is the $L_d$ phase rich in DOPC and Chol. The scale bar corresponds to 10 μm. (For interpretation of the references to colour in this figure legend, the reader is referred to the web version of this article.)

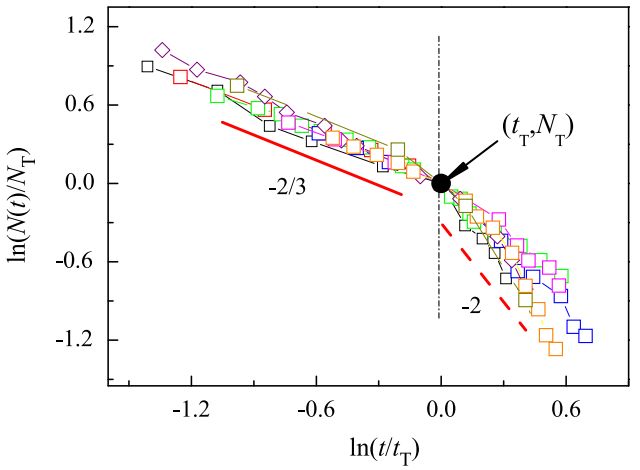


**Fig. 2.** Double-logarithmic plot for the number of domains on the vesicles as a function of time. Each set of data is rescaled by $N_T$ and $t_T$, where $N_T$ is the value of the domain number at the turning point, and $t_T$ is the time corresponding to $N_T$. The solid and the dashed lines have the slopes of $-2/3$ and $-2$, respectively.

an $L_o$ background, which is in clear contrast to the experiments reported in [24–27], where all the systems were $L_o$ domains in an $L_d$ background. Therefore, our results on domain growth are complementary to previous experiments.

To quantify the domain growth dynamics, we can count the number of domains on the vesicles at different times by image analysis. The candidate vesicle should have a diameter larger than 20 μm and number of droplets should be more than 100 in the initial stage (as in Fig. 1). Statistical data of eight such vesicles are shown in Fig. 2, in which the number of domains ($N$) decreases with time ($t$). Although only the domains on the top hemisphere can be seen clearly, statistically, the number of the domains observed should be proportional to the total number of the domains on the vesicle, since the domains are randomly spread on the whole spherical surface [33]. However, we did not investigate the time dependence of the total boundary length or the total area of the dispersed phase, since it is difficult to accurately determine the radius of a droplet from the two-dimensional (2D) projection of a three-dimensional (3D) object under a microscope.

In Fig. 2, all eight $N$–$t$ curves show the same trend: at the beginning the number of domains decreases slowly; after a turning point, it drops suddenly. For clarity, each set of data was rescaled by $N_T$ and $t_T$, in which $N_T$ is the value of the domain number at the turning point, and $t_T$ is the time corresponding to $N_T$. The turning point is marked with a black dot, and two lines with the slope $-2/3$ (solid straight line) and $-2$ (dashed straight line) are added in Fig. 2. For the eight curves presented in Fig. 2, the values of their $t_T$ fall in the range 10–100 s, and there is no significant correlation between $t_T$ and the size of the vesicle. However, it seems that $t_T$ is determined by the domain size, the turning points always appear at the domain size scale around 1 μm (with the reason explained later).

It is interesting to observe that the whole evolution process of the domains on the vesicle surface could be divided into two time regimes: (1), the normal coalescence regime, in which the isolated circular domains form by the coalescence of tiny aggregates, and the growth dynamics follows a scaling relation as $N(t) \sim t^{-2/3}$ (we use the term "normal coalescence" because in this regime the growth exponent $-2/3$ can be explained by assuming conventional Brownian motion of droplet diffusion); (2), the accelerated coalescence regime, in which the domains grow significantly more quickly due to reasons discussed later, and the growth dynamics follows a scaling relation as $N(t) \sim t^{-\beta}$, with $\beta \approx 2$.

We note that to further compare the effect of the fluorescent dyes on the phase separation processes, Chol–BODIPY was added in some experiments instead of TR–DHPE. Chol–BODIPY has the same anchoring part in the membrane as cholesterol does, and is also partitioned mainly in the disordered DOPC-rich ($L_d$) phase. A few sets of the statistical results on domain

number at different times using Chol–BODIPY as the dye have been included in Fig. 2. Therefore, when dyed with two different probes, the phase evolutions are qualitatively the same.

The movement of the domain on the vesicle surface can be modeled as a cylindrical object of radius $R$ and height $h$ (with $R \gg h$) moving in a membrane of thickness $h$ and viscosity $\eta'$, surrounded by fluids on two sides both with viscosity $\eta$. According to the calculation based on the Navier–Stokes equation [34], for $R\eta/h\eta' \gg 1$ (which is the case for the present experiment, with typical material parameters $R \sim 5$ μm, $h \sim 5$ nm, $\eta \sim 10^{-3}$ Pa s, $\eta' \sim 0.1$ Pa s), the dominating drag force on the cylindrical domain comes from the surrounding fluids, and the diffusion constant of the domain is calculated as $D = kT/16\eta R$, where $k$ is the Boltzmann constant and $T$ the temperature. Therefore the viscosity used in the dimensional analysis corresponds to the surrounding fluid.

Thus our system does not corresponding to either the 3D fluids or the exact 2D fluids. Therefore, theoretical analysis on 3D bulk fluids or exact 2D fluids may not be applicable. The nature of hydrodynamic transport in such a quasi-2D membrane may be described as follows: the movement of a domain in the membrane disturbs the surrounding liquid, and then the disturbed surrounding liquid transports a flow to the neighboring domain, which drives its motion. Therefore, the movement of a domain and its neighbor is coupled through the mediation of the surrounding liquid.

At a given temperature $T$, the average velocity scale of such a domain due to thermal diffusion can be estimated as $v_B \sim (kT/m)^{1/2}$, where $m \sim \rho R^2 h$ is the droplet mass and $\rho$ the density of the droplet. On the other hand, the average velocity scale due to hydrodynamic flow (generated by the domain collision) can be estimated from the dimensional analysis applied to $\nabla p = \eta \nabla^2 v_H$, which leads to $v_H \sim \sigma/\eta$, where $\sigma$ is the interfacial tension between the droplet domain and the matrix phase and is related to the line tension: $\gamma = \sigma h$.

In the early stage, the droplet size $R$ is small, and although hydrodynamic flow due to domain collision exists, it cannot compete with the thermal effect because $v_B$ is inversely proportional to $R$. Therefore, in this stage, random diffusion of droplets dominates. The collision between the domains occurs randomly and the growth behavior is dominated by the conventional mechanism of Brownian motion of domain diffusion (the normal coalescence regime). Since the shape deformation of the vesicles is negligible in our experiments, the scaling exponent of the domain growth can be simply deduced as follows [21,22]: if one assumes circular domain shapes, then the average domain radius $R(t) \sim (A_d/N(t))^{1/2}$, and the average diffusion distance when two domains coalesce $l(t) \sim (A_0/N(t))^{1/2} - (A_d/N(t))^{1/2} = [(A_0)^{1/2} - (A_d)^{1/2}]/N^{1/2}(t)$, where $A_0$ is the surface area of the vesicle and $A_d$ is the total area of the droplet phase on the vesicle surface. Since $A_0$ and $A_d$ are constant in phase separation, both $l(t)$ and $R(t)$ are inversely proportional to the square root of $N(t)$, i.e., $l(t) \sim R(t) \sim 1/N^{1/2}(t)$. If one assumes that the diffusion coefficient $D$ follows $D = kT/16\eta R$ due to the hydrodynamic effect of the surrounding liquid, from $D \sim R^{-1}(t)$ and $l^2(t) \sim Dt$, the result will be $R(t) \sim (kT/16\eta)^{1/3} t^{1/3}$ and $N(t) \sim t^{-2/3}$, which is in agreement with the result of our experiment.

For each vesicle, the area fraction occupied by one phase should be a constant. If $L(t)$ stands for the total length of the phase boundaries between the two phases, then $L(t) \sim R(t)N(t)$. By a simple translation, one can easily have $L(t) \sim R^{-1}(t) \sim t^{-1/3}$. These results may be compared to previous theoretical predictions [18–23]. Taniguchi [18] investigated the phase separation of deformable spherical vesicles by coupling the time-dependent Ginzburg–Landau model with Helfrich's elastic membrane model. The time dependence of the total interfacial length $L(t)$ decreased more quickly with the increase of the coupling constant between the composition and curvature of the membrane. However, for the rigid sphere, for which the coupling constant was zero, the time dependence was $L(t) \sim t^{-1/3}$.

After the turning point in Fig. 2, the evolution of domain numbers mostly follows the growth law $N(t) \sim t^{-2}$. The growth behavior in this accelerated coalescence regime cannot be explained by simple Brownian motion of the domains; we speculate that there are other mechanisms that may come into play. To elucidate possible mechanisms in the accelerated coalescence regime, the interface patterns of the domains on the vesicle surface at different times were extracted by image analysis. A typical example of the time evolution of these patterns is shown in Fig. 3. It is easy to observe that during the same period some domains grow rapidly by experiencing a number of collisions, while other domains never collide with another domain. Therefore once a domain experiences a collision-coalescence, it has a much higher probability of a subsequent collision.

A similar phenomenon in binary fluid mixtures was reported by Tanaka [30,31], who proposed a new mechanism called collision-induced collision (CIC) to explain the rapid droplet coarsening. The essence of CIC is that the hydrodynamic flow induced by domain coalescence transports to the neighboring domains and possibly induces another collision. Therefore the collision is not random and the domain growth is accelerated, compared to the growth purely through Brownian motion mechanism. The CIC process in the vesicle is clearly demonstrated in Fig. 4. We observe that before the time at which domain 1 begins to collide with the domain 2, the distance between domains 3 and 4 or 5 and 6 remains stable. Then the coalescence of domains 1 and 2 generates a flow that moves domain 3 toward domain 4. Similarly, the subsequent coalescence of domains 5 and 6 is induced by the collision of domains 3 and 4.

With CIC, the scaling exponent is estimated as follows: the magnitude of the velocity field induced by domain collision can be estimated as $v \sim \sigma/\eta$ by dimensional analysis [31] (a detailed treatment in bulk case can be found in [32,35] and a more relevant analogy for the present vesicle can be found in [34]), where $\sigma$ is the surface tension of the interface between the domain and the matrix ($\sigma$ is related to the line tension as $\gamma = \sigma h$ with $h$ the membrane thickness), and $\eta$ the viscosity of the surrounding fluid (water in this case). If one assumes this velocity field transports the neighboring droplet, the time required for subsequent domain collision, $t_{\text{coll}}$, can be roughly estimated as $t_{\text{coll}} \sim l/v$, where $l$ is the average domain distance. The number of domains $N$ decreases with time as $\mathrm{d}N/\mathrm{d}t \sim -N/t_{\text{coll}}$, combining the relation $l^{-2} = N/S$, where $S$ is the

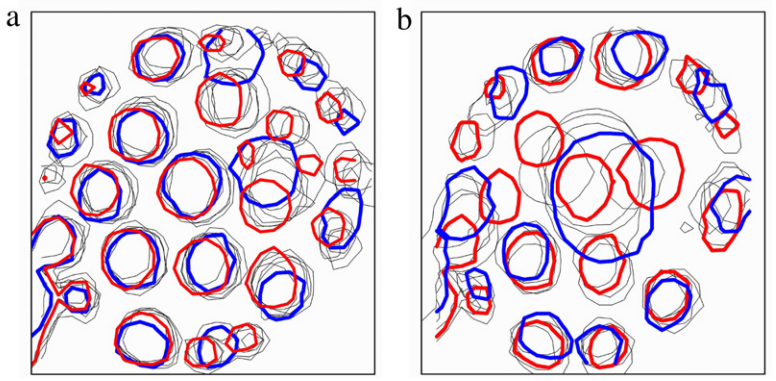


**Fig. 3.** Time evolution of interface pattern on the vesicle surfaces after the ternary mixture was quenched to 15 °C. (a) The interface patterns are superimposed every 2 s from 52 s (red) to 67 s (blue); patterns at times in between are drawn in gray. (b) The interface patterns are superimposed every 2 s from 69 s (red) to 80 s (blue); patterns at times in between are drawn in gray. (For interpretation of the references to colour in this figure legend, the reader is referred to the web version of this article.)

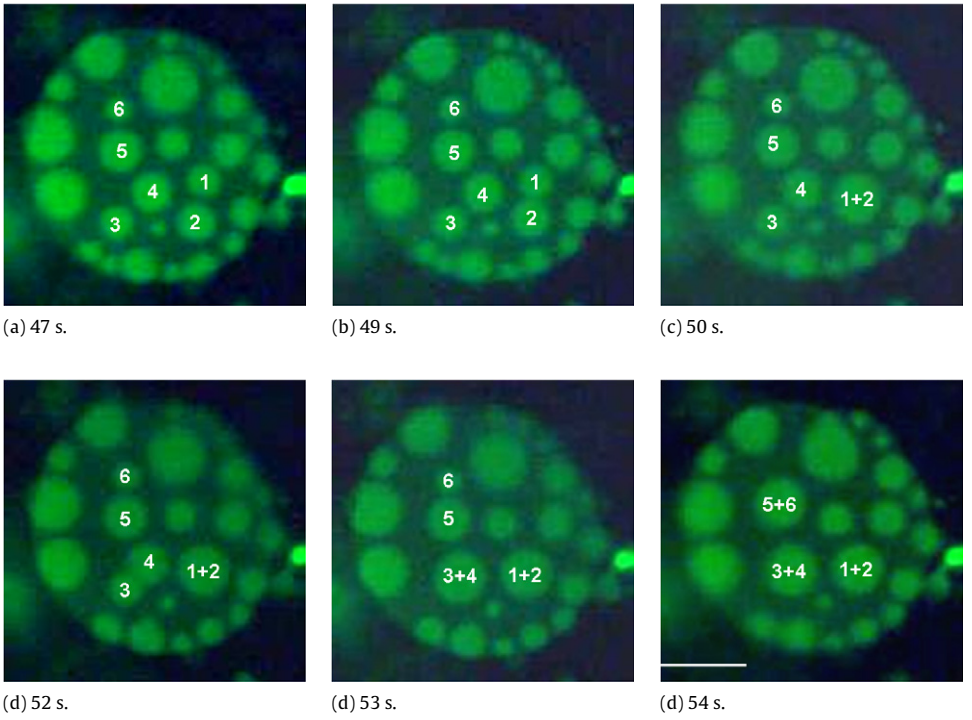


**Fig. 4.** Collision-induced collision on the surface of the vesicle. After the coalescence between domains 1 and 2, the induced hydrodynamic flow generates the multiple collisions between domains 3 and 4, and then 5 and 6. The bright-green phase marked by Chol–BODIPY is the $L_d$ phase rich in DOPC and Chol. The scale bar corresponds to 10 μm. (For interpretation of the references to colour in this figure legend, the reader is referred to the web version of this article.)

(conserved) surface area of the vesicle, one obtains $l \sim vt$. Since the total area of the droplet phase is conserved, one has $l \sim (\pi/\phi_d)^{1/2}R$, and $N(t) \sim A_d/R^2(t)$, where $R$ is the average radius of the droplets and $\phi_d$ the area fraction of the droplets, respectively. With these relations, one obtains $R \sim (\phi_d/\pi)^{1/2}(\sigma/\eta)t$; thus $N(t) \sim t^{-2}$, which means that $\beta = 2$.

The crossover from normal Brownian coagulation to CIC takes place when the Brownian movement of the droplet is dominated by directional hydrodynamic flow (due to domain collision), i.e., when $v_H > v_B$. Taking typical values of material parameters, $h \sim 5$ nm, $\eta \sim 10^{-3}$ Pa s, $\gamma \sim 0.1$pN, $\rho \sim 500$ kg m$^{-3}$, and $T \sim 300$ K, the size scale of the droplet at the crossover is estimated to be around 2 μm, which is reasonably consistent with our experimental observation. With the droplet growth dynamics $R^2 \sim (kT/16\eta R)t$, taking $R \sim 2$ μm, the magnitude of the turning time $t_T$ is estimated to be 20 s, which is also qualitatively in agreement with the experiment.

Finally, we compare our experimental results with the results reported recently by Saeki et al. [24], Yanagisawa et al. [25], Ursell et al. [26], and Semrau et al. [27]. All these groups used ternary mixtures of DPPC/DOPC/Chol to study the domain

growth dynamics on the fluid vesicles, except the last group, which used an SM/DOPC/Chol mixture. They all reported the emergence of a repulsive force between capped domains, resulting in a dynamically trapped state in which domain coalescence was suppressed. Their results immediately raise an interesting question: why in a similar ternary mixture we have observed normal and accelerated domain growth? After a careful inspection of the experimental conditions used in all the experiments, we have found an important difference between our experiment and the others: in our system, we typically observe many $L_d$ droplet domains in an $L_o$ background (see Figs. 1 and 4); however, in all other earlier experiments, the droplets are the $L_o$ phase, while the continuous matrix is the $L_d$ phase [24–27]. Since the $L_o$ matrix phase is much stiffer than the $L_d$ domains (typically the ratio of their bending moduli can be greater than 4) [36], we speculate this may be the reason why we did not observe the slowing down of domain coalescence.

Previous experiments described a slowing down of domain coalescence [24–27] due to membrane-mediated interactions. The essence of this interaction is that there must exist partially budded domains that bend their neighboring (matrix) membrane, which in turn leads to an elastic energy barrier that hinders the further approaching of these domains. According to the measurement in [26], which is a system of $L_o$ droplets in an $L_d$ matrix phase, this coalescence barrier between budded domains is estimated to be ∼5–10 kT. In our case, however, the matrix is the $L_o$ phase, which is more difficult to be bent, since the bending modulus of the $L_o$ phase is much higher than that of the $L_d$ phase. We thus speculate that in our system no significant (local) bending of the matrix $L_o$ phase, caused by the budded $L_d$ domains, would happen, as evidenced by the observation in the experiment (Figs. 1 and 4). This gives the hydrodynamics a chance to accelerate the domain coalescence. However, the underlying physics is not clear in the present stage. Further study is needed to clarify the effect of modulus difference on the domain growth dynamics.

## 4. Conclusion

In summary, we have investigated the domain growth dynamics in spherical vesicles with model mixtures of BSM/DOPC/Chol by quenching the ternary mixture from the one-phase region to the liquid–liquid coexistence region. Two fluorescence probes, TR–DHPE and Chol–BODIPY, which both partitioned in the DOPC-rich $L_d$ phase, were added to improve the phase contrast in the optical images and to compare possible effects of the probe molecules. In our system, we observed $L_d$ droplets in an $L_o$ background; therefore the system was in a different state compared to previous experiments which reported slowing down of domain coalescence. We however recognized two distinct time regimes of the domain growth: (1) in the early stage, the number of domains on the vesicle surface decreases with time as $N(t) \sim t^{-2/3}$, as predicted in previous theoretical analysis and numerical simulations; (2) in the late stage, the hydrodynamics plays a more important role in the domain growth, resulting a growth law $N(t) \sim t^{-\beta}$, with $\beta \approx 2$. The rapid decreasing trend of the domain numbers may be explained by the collision-induced collision mechanism, which was proposed earlier to discuss rapid coarsening mechanisms in binary fluid mixtures. Meanwhile, our experiments showed that the domain growth dynamics is not affected by what dye is used.

## Acknowledgements

We are grateful for the financial support from the National Basic Research Program of China (Grant No. 2005CB623800) and National Natural Science Foundation of China (Grants No. 20625413 and No. 20874021).

## References

[1] K. Simons, E. Ikonen, Nature 387 (1997) 569.
[2] W.H. Binder, V. Barragan, F.M. Menger, Angew. Chem. Int. Ed. 42 (2003) 5802.
[3] K. Simons, D. Toomre, Nature Reviews: Molecular Cell Biology 1 (2000) 31.
[4] S. Semrau, T. Schmidt, Soft Matter 5 (2009) 3174.
[5] L. Bagatolli, P.B.S. Kumar, Soft Matter 5 (2009) 3234.
[6] S.L. Veatch, S.L. Keller, Biophys. J. 85 (2003) 3074.
[7] R.F.M. de Almeida, A. Fedorov, M. Prieto, Biophys. J. 85 (2003) 2406.
[8] S.L. Veatch, S.L. Keller, Phys. Rev. Lett. 94 (2005) 148101.
[9] G. Orädd, G. Lindblom, P.W. Westerman, Biophys. J. 83 (2002) 2702.
[10] A. Filippov, G. Orädd, G. Lindblom, Biophys. J. 86 (2004) 891.
[11] A. Filippov, G. Orädd, G. Lindblom, Biophys. J. 90 (2006) 2086.
[12] T. Baumgart, S.T. Hess, W.W. Webb, Nature 425 (2003) 821.
[13] T. Baumgart, S. Das, W.W. Webb, J.T. Jenkins, Biophys. J. 89 (2005) 1067.
[14] R. Lipowsky, J. Phys. II France 2 (1992) 1825.
[15] F. Jülicher, R. Lipowsky, Phys. Rev. Lett. 70 (1993) 2964.
[16] M. Yanagisawa, M. Imai, T. Taniguchi, Phys. Rev. Lett. 100 (2008) 148102.
[17] S. Rozovsky, Y. Kaizuka, J.T. Groves, J. Am. Chem. Soc. 127 (2005) 36.
[18] T. Taniguchi, Phys. Rev. Lett. 76 (1996) 4444.
[19] P.B.S. Kumar, M. Rao, Mol. Cryst. Liq. Cryst. 288 (1996) 105.
[20] P.B.S. Kumar, M. Rao, Phys. Rev. Lett. 80 (1998) 2489.
[21] P.B.S. Kumar, G. Gompper, R. Lipowsky, Phys. Rev. Lett. 86 (2001) 3911.
[22] M. Laradji, P.B.S. Kumar, Phys. Rev. Lett. 93 (2004) 198105.
[23] M. Laradji, P.B.S. Kumar, J. Chem. Phys. 123 (2005) 224902.
[24] D. Saeki, T. Hamada, K. Yoshikawa, J. Phys. Soc. Japan 75 (2006) 013602.

[25] M. Yanagisawa, M. Imai, T. Masui, S. Komura, T. Ohta Biophys. J. 92 (2007) 115.
[26] T.S. Ursell, W.S. Klug, R. Phillips, Proc. Natl. Acad. Sci. USA 106 (2009) 13301.
[27] S. Semrau, T. Idema, T. Schmidt, C. Storm, Biophys. J. 96 (2009) 4906.
[28] L. Li, X.Y. Liang, M.Y. Lin, F. Qiu, Y.L. Yang, J. Am. Chem. Soc. 127 (2005) 17996.
[29] P.G. Saffman, M. Delbrück, Proc. Natl. Acad. Sci. USA 72 (1975) 3111.
[30] H. Tanaka, Phys. Rev. Lett. 72 (1994) 1702.
[31] H. Tanaka, J. Chem. Phys. 105 (1996) 10099.
[32] H. Tanaka, J. Chem. Phys. 107 (1997) 3734.
[33] A.R. Bausch, M.J. Bowick, A. Cacciuto, A.D. Dinsmore, M.F. Hsu, D.R. Nelson, M.G. Nikolaides, A. Travesset, D.A. Weitz, Science 299 (2000) 8738.
[34] B.D. Hughes, B.A. Pailthorpe, L.R. White, J. Mech. Fluids 110 (1981) 349.
[35] V.G. Karpov, Phys. Rev. Lett. 75 (1995) 2702.
[36] S. Semrau, T. Idema, L. Holtzer, T. Schmidt, C. Storm, Phys. Rev. Lett. 100 (2008) 088101.